ResearchGate

See discussions, stats, and author profiles for this publication at: https://www.researchgate.net/publication/51669513

Plasmonic Nanoparticle Chain in a Light Field: A Resonant Optical Sail

ARTICLE *in* NANO LETTERS · SEPTEMBER 2011

Impact Factor: 13.59 · DOI: 10.1021/nl201996t · Source: PubMed

CITATIONS
3

READS
43

3 AUTHORS:

Silvia Albaladejo
Conento
15 PUBLICATIONS **279** CITATIONS

SEE PROFILE

Juan José Sáenz
Donostia International Physics Center
227 PUBLICATIONS **4,618** CITATIONS

SEE PROFILE

Manuel Ignacio Marques
Universidad Autónoma de Madrid
87 PUBLICATIONS **694** CITATIONS

SEE PROFILE

Available from: Manuel Ignacio Marques
Retrieved on: 03 February 2016

NANO LETTERS

LETTER

pubs.acs.org/NanoLett

Plasmonic Nanoparticle Chain in a Light Field: A Resonant Optical Sail

Silvia Albaladejo,[†,‡] Juan José Sáenz,[†,‡,§] and Manuel I. Marqués*[∥,‡]

[†]Departamento de Física de la Materia Condensada, Universidad Autónoma de Madrid, 28049 Madrid, Spain

[‡]Instituto"Nicolás Cabrera", Universidad Autónoma de Madrid, 28049 Madrid, Spain

[§]Donostia International Physics Center (DIPC), Paseo Manuel Lardizabal 4, 20018 Donostia-San Sebastian, Spain

[∥]Departamento de Física de Materiales, Universidad Autónoma de Madrid, 28049 Madrid, Spain

ABSTRACT: Optical trapping and driving of small objects has become a topic of increasing interest in multidisciplinary sciences. We propose to use a chain made of metallic nanoparticles as a resonant light sail, attached by one end point to a transparent object and propelling it by the use of electromagnetic radiation. Driving forces exerted on the chain are theoretically studied as a function of radiation's wavelength and chain's alignments with respect to the direction of radiation. Interestingly, there is a window in the frequency spectrum in which null−torque equilibrium configuration, with minimum geometric cross section, corresponds to a maximum in the driving force.

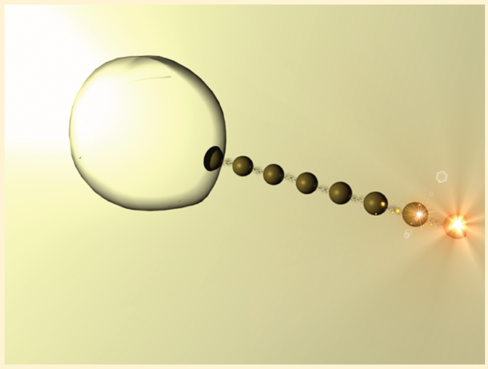

KEYWORDS: Optical forces, torque, plasmonic chains, gold nanoparticles, optical resonances

The ability of light to exert forces has been known for almost five hundred years, when deflection of comet tails by the sun's rays was detected by Kepler; however it was not until 1970 when motion of small dielectric particles was first controlled using laser beams.[1] Since then, optical manipulation including driving and trapping of small particles by using appropriate light fields[2−4] has become a mainstay of research in physics and biology.[5−10]

These optical forces are often insufficient to manipulate biological macromolecules alone, and a common approach is to attach them to submicrometer highly polarizable dielectric spheres or metallic nanoparticles that serve as handles.[7−15] At certain wavelengths, the large extinction cross section due to surface plasmon resonances makes them act more like optical "sails" for driving than like handles. While the optical forces acting on state of the art micrometer-sized colloidal spheres can be of the order or larger than those on resonant nanoparticles, the drag forces, a key issue in viscous biological environments, are strongly reduced for nanometer size particles. Our purpose here is to explore the possibility of using these plasmonic nanoparticles as building blocks of complex resonant optical sails at the nanoscale.

Metallic nanoparticles can be precisely positioned periodically on self-assembled DNA,[16−20] using polymers as a template for assembly or peptide-based methods,[21,22] leading to one-dimensional chains. The study of the optical properties of linear chains of plasmonic nanoparticles received considerable interest in the context of light transport in subwavelength optical guiding structures.[23−34] At collective plasmon resonances, the plasmonic nanoparticle chain (PNC) present a huge extinction cross section. A chain made of metallic nanoparticles could then work as a light sail, attached by one end point to a transparent object and propelling it by the use of electromagnetic radiation.

In this work we study a light sail made up of a chain of metallic nanoparticles. We theoretically characterize the net driving force and torque felt by the gold nanoparticle chain, attached at one end point to an object, under plane wave illumination for different configurations and wavelengths. Results found are explained in terms of geometrical and plasmonic resonances. Near collective (geometrical) resonances, radiation pressure is found to be strongly increased when both sail and direction of radiation are parallel to each other. In contrast with day life intuition, we show how there is no need to hold any torque on the light sail in order to obtain a net driving force different from zero at the equilibrium configuration on an object attached to the PNC's end point.

To make the optical force study, we will consider a chain made up of $N_p = 100$ gold nanoparticles of $a = 50$ nm radius and distance between nanoparticles $D = ma$ (m being an integer number) lying on the $X-Y$ plane. The chain is embedded in water and free to rotate around a Z axis that crosses the chain's end point. A Z linearly polarized beam of laser light with density power $P = 4.5 \times 10^5 \mathrm{W/cm^2}$ illuminates the chain. Direction of propagation of the incident radiation is always pointing toward the X direction ($\mathbf{k} = k\mathbf{i}$) as sketched in Figure 1. The angle between the incident electromagnetic field and the metal chain (θ) goes from $\theta = 0$ to $\theta = 2\pi$, corresponding $\theta = 0$ to the configuration with chain's axis perpendicular to the propagation of the electromagnetic radiation (see Figure 1). Angles going clockwise, will be considered as positive.

First theoretical analysis about light forces are due to Maxwell who showed that the momentum flux in a beam of light is

Received: June 14, 2011
Revised: September 16, 2011

ACS Publications © XXXX American Chemical Society

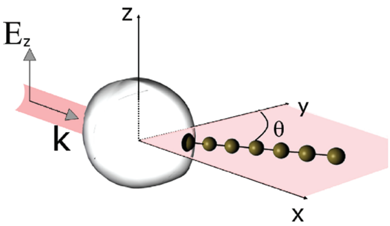

Figure 1. Sketch representing a light sail composed of a gold nanoparticle chain. Gold nanoparticles inside the chain are separated by a distance D. Sail is illuminated by a electromagnetic plane wave propagating in the X direction and polarized in the Z direction, producing a driving force on an attached nanoscopic object. Angle is defined with respect to the Y axes.

proportional to the intensity and can be transferred to illuminated objects pushing the object along the direction of propagation. Apart from this pressure force there is a gradient force along the gradient of the field intensity and a spin force along the curl of the angular momentum.[4] Time averaged total optical force acting on a particle with polarizability ($\alpha = \alpha' + i\alpha''$) and extintion cross section $\sigma = k\alpha''$ is given by

$$\mathbf{F} = \alpha'\{\nabla\langle U\rangle\} + \sigma\left\{\frac{n}{c}\langle\mathbf{S}\rangle\right\} + \sigma\left\{\frac{c}{n}\nabla\times\langle\mathbf{L}_{\mathrm{S}}\rangle\right\} \tag{1}$$

being n the refractive index of the dielectric medium, U the field's intensity, $\mathbf{S}$ the Poynting's vector, and $\mathbf{L}_{\mathrm{S}}$ the spin angular momentum of the electromagnetic field. At visible frequencies nanosized particles are very small compared with the incident wavelength, so a constant field inside the nanoparticle may be admitted and particle's polarizability can be approximated by[35]

$$\alpha = \frac{\alpha_0}{1 - i\alpha_0 k^3/(6\pi)} \tag{2}$$

$$\alpha_0 = 4\pi a^3 \frac{\varepsilon_{\mathrm{g}}(\omega) - \varepsilon}{\varepsilon_{\mathrm{g}}(\omega) + 2\varepsilon}$$

where $\varepsilon_{\mathrm{g}}(\omega)$ is the frequency dependent macroscopic relative permittivity of the metallic nanoparticle and ε the macroscopic relative permittivity of the dielectric medium.

The total time averaged force acting on a nanoparticle may be computed by calculating the field and the gradient of the field on each nanoparticle[36]

$$\mathbf{F} = (1/2)\mathrm{Re}\left(\sum_i p_i \nabla \mathbf{E}_i^*\right) \tag{3}$$

with $p_i = \varepsilon_0\varepsilon\alpha E_i$ and $i = x,y,z$.

The Z-polarized electric field acting on each spherical nanoparticle will be the sum of the plane wave illumination $\mathbf{E}_0(\mathbf{r})$ and the scattering coming from the rest of nanoparticles in the same chain

$$\mathbf{E}(\mathbf{r}_n) = \mathbf{E}_0(\mathbf{r}_n) + \alpha \sum_{n\neq m} G(\mathbf{r}_n, \mathbf{r}_m)\mathbf{E}(\mathbf{r}_m) \tag{4}$$

We consider the dipole approximation

$$G(\mathbf{r}_n, \mathbf{r}_m) = \frac{1}{4\pi}\left(\frac{k^2}{r_{n,m}} - \frac{1}{r_{n,m}^3} + \frac{ik}{r_{n,m}^2}\right)\mathrm{e}^{ikr_{n,m}} \tag{5}$$

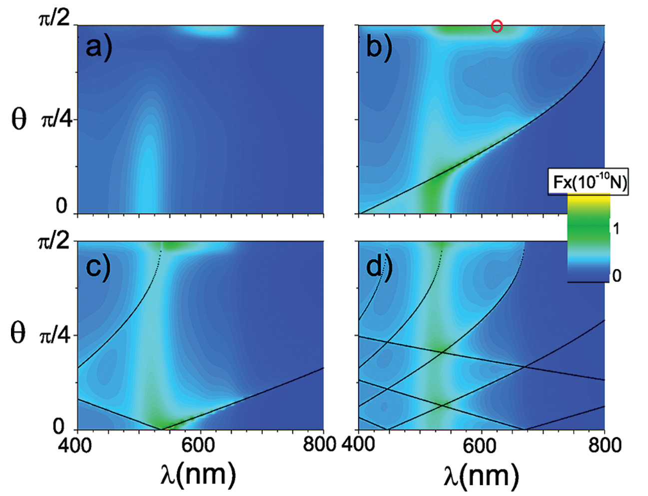

Figure 2. Optical force map for (a) $D = 3a$, (b) $D = 6a$, (c) $D = 8a$, and (d) $D = 20a$. Black lines correspond with analytical values of $\theta_{\max}$ from eq 11. Red circle corresponds to the force at $\lambda = 625$ nm and $\theta = \pi/2$ (see text).

being $r_{n,m}$ the distance between "n" and "m" nanoparticles. Fields and optical forces are obtained by solving this set of $N_p \times N_p$ equations.

In Figure 2 we have plotted a map of the optical driving force (force in the X direction) when changing wavelength and θ for four different values of the distance between particles. Note how maximum on the "pushing" force is not obtained at $\theta = 0$ (which is the expected value for a regular wind sail) but at a value $\theta_{\max}$ that strongly depends on laser's wavelength and distance between particles. In general, for any angle, large values of the forces are observed at $\lambda \sim 520$ nm. There is also a region of wavelengths where strong driving forces are obtained for $\theta \sim \pi/2$.

The increment of the force at $\lambda \sim 520$ nm is related to the plasmonic resonance of the single's gold particle extinction cross section. This resonance is associated with the polarizability and shows up for frequency value's with $\varepsilon_{\mathrm{g}}(\omega) = -2\varepsilon$.

Large vales of the driving force are also obtained at other wavelength values far from this resonance. In order to understand this geometrical type of resonances due to the scattering between the different particles, we have analytically analyzed the problem of an infinite chain illuminated with the plane wave of amplitude E_0.

For an infinite chain

$$\mathbf{E}(r_n) = \frac{\mathbf{E}_0\mathrm{e}^{ikx_n}}{1 - \alpha G(k)} \tag{6}$$

with

$$G(k) = \sum_{n\neq m} G(\mathbf{r}_n, \mathbf{r}_m)\mathrm{e}^{ik(x_m - x_n)} \tag{7}$$

Due to the small value of the polarizability in eq 6, $G(k)$ must be large in order to obtain non-neglightable electric fields and forces. Taking into account the equivalence between all particles in the infinity chain and considering only the logarithmic divergent term (i.e., long-range far-field interactions) we get

$$G(k) \sim \frac{k^2}{4\pi D}\sum_{n=1}^{\infty}\left(\frac{\mathrm{e}^{iknD(1+\sin(\theta))}}{n} + \frac{\mathrm{e}^{iknD(1-\sin(\theta))}}{n}\right) \tag{8}$$

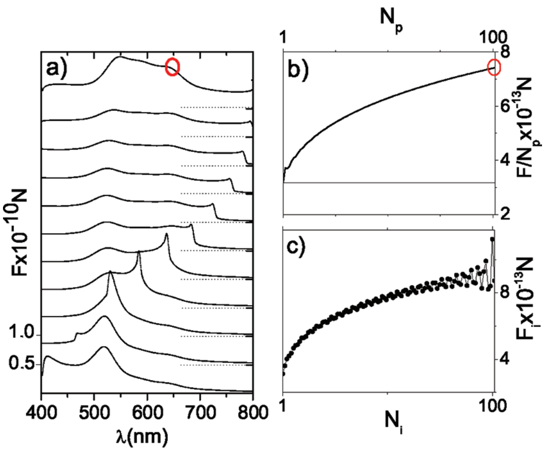

Figure 3. (a) Driving force vs wavelength at different equispaced angles from $\theta = 0$ (lower curve) to $\theta = \pi/2$ (upper curve) (extracted from the force map in Figure 2b). For the sake of clarity, individual curves are shifted vertically (horizontal dotted lines indicates the zero force value for each curve). (b) Normalized total driving force (F/N_p at ($\theta = \pi/2$)) vs the total number of particles, N_p in the chain at $\lambda = 625$ nm and $D = 6a$. Horizontal line corresponds to the case of noninteracting particles. (c) Driving force F_i on each nanoparticle, $N_i = 1, ..., N_p$, for a chain with $N_p = 100$. The chain is illuminated from the left, i.e., particle $N_i = 1$ is the closest to the light source. The total driving force for $N_p = 100$, $F = \sum_{i=1}^{N_p} F_i$ corresponds to the red circle in (a), (b), and in Figure 2b).

which may be rewritten with this relation

$$\sum_{m>0} \frac{e^{imB}}{m} = -\ln[1 - e^{iB}] \tag{9}$$

as[23−27]

$$G(k) \sim -\frac{k^3}{4\pi}\frac{1}{kD}\ln[2e^{ikD}(\cos(kD) - \cos(kD \sin\theta))] \tag{10}$$

so (the real part of) $G(k)$ will diverge at angles given by $\cos(kD \sin\theta_{max}) = \cos(kD)$, i.e.

$$k \sin\theta_{max} = \pm\frac{2\pi m}{D} \mp k \tag{11}$$

or

$$\theta_{max} = a\sin\left(\pm\frac{2\pi c}{D\sqrt{\varepsilon}\omega}m \mp 1\right)$$

with $m = 0, 1, 2, 3, ...$ This condition corresponds to the onset of propagating diffracted modes. Similar conditions appear in the analysis of geometrical dynamic resonances in hole arrays and gratings.[37,38] As long as the real part of the polarizability remains small and positive, the resonances should take place very close to the geometrical condition given by eq 11 which only depends on the ratio $\lambda/D = 2\pi/(kD)$. We have plotted these values for θ_{max} together with the results obtained for the finite chain (see Figure 2). Note how θ_{max} values obtained from equation eq 11 are close to the resonant peaks obtained from the numerical results. Since the resonant condition has been derived without including near-field interactions, resonances at the angles given by eq 11 are due to collective constructive interference of the long-range (radiative) scattered fields. In contrast with the $m \neq 0$ geometric conditions, the $m = 0$ condition at $\theta_{max} \approx \pi/2$ does not depend on λ/D. These resonances are of particular interest since they correspond to large driving forces with minimum geometric cross section.

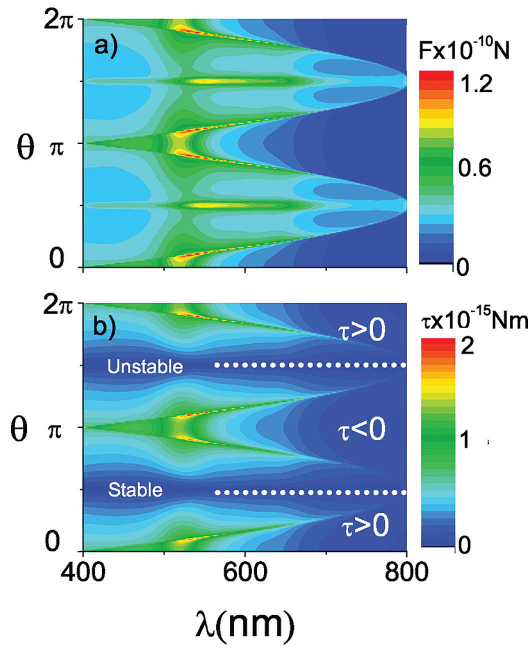

Figure 4. (a) Forces and (b) modulus of the torque's map for $D = 6a$.

In Figure 3a we plotted the force versus wavelength at different angles (extracted from the force map in Figure 2b). This figure summarizes the different resonant forces on the nanoparticle chain: At $\theta \approx 0$, the broad resonance around $\lambda = 520$ nm ($\approx\pm 25$ nm) corresponds to the single particle localized plasmon resonance while the peak at lower wavelengths corresponds to the $m = 1$ geometric (collective) resonance signaling the onset of the first diffracted beam. As the angle increases, the localized plasmon peak decreases and the geometric resonance shifts to the red (following the black line in Figure 2b) becoming narrower at long wavelengths (width $\approx \pm 10$ nm), and eventually disappearing into a force step edge which separates the force map in two well-defined regions. In the region corresponding to $\theta > \theta_{max}(\lambda/D)$ there is a constant background, due to the additional contribution of the first diffracted mode to the total force.

As we approach $\theta = \pi/2$, there is a new, very broad, peak (width $\approx \pm 75$ nm) that corresponds to the $m = 0$ resonance. The collective nature of this resonance is illustrated in Figure 3b where we show how the force per particle F/N_p increases with the total number of particles in the chain N_P. Whithin this resonance region, and in analogy with previously reported field enhancement effects,[39] the analysis of the optical forces on each nanoparticle clearly indicates a force enhancement at the extremity of the finite chain (see Figure 3c). The asymmetry of the force field along the chain is due to a cumulative resonant effect coming from the interference of the long-range (radiative) scattered fields.[40] Interestingly, this asymmetry in the force field would induce an effective tension along the wire that would work against steric fluctuations helping to keep the straight shape of the chain. This opens intriguing possibilities to optically tune the effective persistence length of the chain.

In order to obtain a complete view of the mechanical response of the nanometric system, it is of interest to analyze other issues as the alignment and rotations of the chain.[41] We have then calculated the total torque over the chain with $D = 6a$ when attached to an end point at $r = r_1$. Torque over the chain is defined as

$$\tau = \sum_{i=2}^{N_p} \mathbf{F}(\mathbf{r}_i) \times (\mathbf{r}_i - \mathbf{r}_1) \tag{12}$$

We plot in Figure 4 the driving force exerted over the chain and the modulus of the torque. Equilibrium configuration in a mechanical system corresponds to a stable null torque which produces no driving force at all. However in the light sail under study, this equilibrium configuration at $\theta = \pi/2$ (nanochain parallel to incident radiation) produces a noticeable driving force, due to the cumulative plasmon enhancement effect, different from zero. In this way, with no need to hold any torque at all, an enhanced driving effect over the object attached to the light sail is obtained.

Finally, we discuss some possible issues concerning the experimental realization of an optical sail. Achieving optimal performance requires tuning the chain resonance near the light frequency (wavelength) of reasonably high-power lasers. Chains made of metal nanoshells, whose optical resonance can be "designed in" in a controlled manner,[11] would be an alternative for tuning the localized plasmon resonance frequency. Geometrical resonances could be tailored by control of the distance between particles. First steps to control the interparticle spacing on peptide chains[21,22] have been recently reported in the 10 nm range. A combination of chemical self-assembled methods together with nanolitrographic tools could be an alternative to increase the spacing to values closer to the light wavelength.

To conclude, we have computed the total force and torque exerted on a chain made of gold nanoparticles in a plane wave light field. Maxima in the drag force can be obtained when the chain is aligned with the incident flow, exposing minimum geometrical cross section. This counterintuitive behavior is explained in terms of collective plasmon resonances. Nanoscale optical sails could open new perspectives in optical dragging and manipulation of macromolecular assemblies of interest in physical chemistry and biology.

AUTHOR INFORMATION

Corresponding Author
*E-mail: manuel.marques@uam.es.

ACKNOWLEDGMENT

This work has been supported by the Spanish MICINN Consolider NanoLight (CSD2007-00046), FIS2009-13430-C02-02 Projects and by the Comunidad de Madrid Microseres Program (S2009/TIC-1476).

REFERENCES

(1) Ashkin, A. *Phys. Rev. Lett.* **1970**, *24*, 156.
(2) Ashkin, A.; Dziedzic, J. M.; Yamane, T. *Nature* **1987**, *330*, 769–771.
(3) Ashkin, A.; Dziedzic, J. *Science* **1987**, *235*, 1517–1520.
(4) Albaladejo, S.; Marqués, M. I.; Laroche, M.; Sáenz, J. J. *Phys. Rev. Lett.* **2009**, *102*, 113602.
(5) Grier, D. *Nature* **2003**, *424*, 810–816.
(6) Neuman, K. C.; Block, S. M. *Rev. Sci. Instrum.* **2004**, *75*, 2787.
(7) Svoboda, K.; Schmidt, C.; Schnapp, B.; Block, S. *Nature* **1993**, *365*, 721–727.
(8) Moffitt, J. R.; Chemla, Y. R.; Smith, S. B.; Bustamante, C. *Annu. Rev. Biochem.* **2008**, *77*, 205–228.
(9) Svoboda, K.; Block, S. *Annu. Rev. Biophys. Biomol. Struct.* **1994**, *23*, 247–285.
(10) Mehta, A.; Rief, M.; Spudich, J.; Smith, D.; Simmons, R. *Science* **1999**, *283*, 1689–1695.
(11) Oldenburg, S.; Averitt, R.; Westcott, S.; Halas, N. *Chem. Phys. Lett.* **1998**, *288*, 243–247.
(12) Kelly, K.; Coronado, E.; Zhao, L.; Schatz, G. *J. Phys. Chem. B* **2003**, *107*, 668–677.
(13) Jain, P. K.; Huang, X.; El-Sayed, I. H.; El-Sayed, M. A. *Acc. Chem. Res.* **2008**, *41*, 1578–1586.
(14) Edidin, M.; Kuo, S.; Sheetz, M. *Science* **1991**, *254*, 1379–1382.
(15) Svoboda, K.; Block, S. *Opt. Lett.* **1994**, *19*, 930–932.
(16) Seeman, N. *Nature* **2003**, *421*, 427–431.
(17) Deng, Z.; Mao, C. *Nano Lett.* **2003**, *3*, 1545–1548.
(18) Park, S.; Taton, T.; Mirkin, C. *Science* **2002**, *295*, 1503–1506.
(19) Warner, M. G.; Hutchison, J. E. *Nat. Mater.* **2003**, *2*, 272–277.
(20) Li, H.; Park, S. H.; Reif, J. H.; LaBean, T. H.; Yan, H. *J. Am. Chem. Soc.* **2004**, *126*, 418–9.
(21) Sardar, R.; Shumaker-Parry, J. S. *Nano Lett.* **2008**, *8*, 731–736.
(22) Chen, C.-L.; Rosi, N. L. *J. Am. Chem. Soc.* **2010**, *132*, 6902–6903.
(23) Quinten, M.; Leitner, A.; Krenn, J.; Aussenegg, F. *Opt. Lett.* **1998**, *23*, 1331–1333.
(24) Citrin, D. *Nano Lett.* **2004**, *4*, 1561–1565.
(25) Citrin, D. *Nano Lett.* **2005**, *5*, 985–989.
(26) Brongersma, M.; Hartman, J.; Atwater, H. *Phys. Rev. B* **2000**, *62*, 16356–16359.
(27) Guillon, M. *Opt. Express* **2006**, *14*, 3045–3055.
(28) Maier, S.; Brongersma, M.; Kik, P.; Meltzer, S.; Requicha, A.; Atwater, H. *Adv. Mater.* **2001**, *13*, 1501–1505.
(29) Maier, S.; Kik, P.; Atwater, H. *Appl. Phys. Lett.* **2002**, *81*, 1714–1716.
(30) Maier, S.; Kik, P.; Atwater, H. *Phys. Rev. B* **2003**, *67*, 205402.
(31) Koenderink, A. F.; Polman, A. *Phys. Rev. B* **2006**, *74*, 033402.
(32) Zhao, L.; Kelly, K.; Schatz, G. *J. Phys. Chem. B* **2003**, *107*, 7343–7350.
(33) Sweatlock, L.; Maier, S.; Atwater, H.; Penninkhof, J.; Polman, A. *Phys. Rev. B* **2005**, *71*, 235408.
(34) Li, H.; Liu, Q.; Xie, S.; Zhou, X.; Xia, H.; Zhou, R. *Solid State Commun.* **2008**, *149*, 239–242.
(35) Draine, B. *Astrophys. J.* **1988**, *333*, 848–872.
(36) Chaumet, P.; Nieto-Vesperinas, M. *Opt. Lett.* **2000**, *25*, 1065–1067.
(37) de Abajo, F. J. C.; Gómez-Medina, R.; Sáenz, J. J. *Phys. Rev. E* **2005**, *72*, 016608.
(38) Gómez-Medina, R.; Laroche, M.; Sáenz, J. J. *Opt. Express* **2006**, *14*, 3730–3737.
(39) Ghenuche, P.; Cormack, I.; Badenes, G.; Loza-Alvarez, P.; Quidant, R. *Appl. Phys. Lett.* **2007**, *90*, 041109.
(40) de Waele, R.; Koenderink, A. F.; Polman, A. *Nano Lett.* **2007**, *7*, 2004–2008.
(41) Tong, L.; Miljković, V. D.; Käll, M. *Nano Lett.* **2010**, *10*, 268–273.